Title
Sustained MEK inhibition abrogates myeloproliferative disease in Nf1 mutant mice.

Journal
Journal of Clinical Investigation, 123(1)

Authors
Chang, Tiffany
Krisman, Kimberly
Theobald, Emily
et al.

Publication Date
2013

DOI
10.1172/JCI63193

Peer reviewed

Sustained MEK inhibition abrogates myeloproliferative disease in *Nf1* mutant mice

Tiffany Chang,[1] Kimberly Krisman,[1] Emily Harding Theobald,[1] Jin Xu,[1] Jon Akutagawa,[1] Jennifer O. Lauchle,[1] Scott Kogan,[2,3] Benjamin S. Braun,[1] and Kevin Shannon[1,3]

[1]Department of Pediatrics, [2]Department of Laboratory Medicine, and [3]Helen Diller Family Comprehensive Cancer Center, UCSF, San Francisco, California, USA.

Children with neurofibromatosis type 1 (NF1) are predisposed to juvenile myelomonocytic leukemia (JMML), an aggressive myeloproliferative neoplasm (MPN) that is refractory to conventional chemotherapy. Conditional inactivation of the *Nf1* tumor suppressor in hematopoietic cells of mice causes a progressive MPN that accurately models JMML and chronic myelomonocytic leukemia (CMML). We characterized the effects of *Nf1* loss on immature hematopoietic populations and investigated treatment with the MEK inhibitor PD0325901 (hereafter called 901). Somatic *Nf1* inactivation resulted in a marked expansion of immature and lineage-committed myelo-erythroid progenitors and ineffective erythropoiesis. Treatment with 901 induced a durable drop in leukocyte counts, enhanced erythropoietic function, and markedly reduced spleen sizes in mice with MPN. MEK inhibition also restored a normal pattern of erythroid differentiation and greatly reduced extramedullary hematopoiesis. Remarkably, genetic analysis revealed the persistence of *Nf1*-deficient hematopoietic cells, indicating that MEK inhibition modulates the proliferation and differentiation of *Nf1* mutant cells in vivo rather than eliminating them. These data provide a rationale for performing clinical trials of MEK inhibitors in patients with JMML and CMML.

Introduction

Neurofibromatosis type 1 (NF1) is a familial cancer syndrome caused by mutations in the *NF1* gene (1). Children with NF1 are at markedly increased risk of myeloid malignancies, particularly juvenile myelomonocytic leukemia (JMML), a relentless myeloproliferative neoplasm (MPN) characterized by leukocytosis, dysplasia, thrombocytopenia, and malignant organ infiltration (2). HSC transplantation (HSCT) cures approximately 50% of patients (2).

NF1 encodes neurofibromin, a GTPase-activating protein (GAP) that negatively regulates Ras signaling (1). Consistent with this biochemical activity, *NF1* functions as a tumor-suppressor gene in JMML (3), and diseased BM cells exhibit aberrant Raf/MEK/ERK signaling (4). The association with NF1 implicated hyperactive Ras in the pathogenesis of JMML, and mutations in genes encoding components of Ras signaling networks were subsequently identified in approximately 90% of JMML patients (2). Thus, JMML is fundamentally a disease of hyperactive Ras.

Mx1-Cre;Nf1$^{flox/flox}$ mice develop an MPN with many similarities to JMML (5). Insertional mutagenesis in this strain cooperates with *Nf1* inactivation to drive progression to acute myeloid leukemia (AML) (6), which models transformation in patients with JMML and chronic myelomonocytic leukemia (CMML) (7). The Raf/MEK/ERK effector pathway is an appealing therapeutic target in JMML, CMML, and AML (5). We previously evaluated CI-1040, a "first generation" MEK inhibitor, in *Mx1-Cre;Nf1*$^{flox/flox}$ mice with MPN and in recipients that were transplanted with *Nf1* mutant AML cells (6). Whereas CI-1040 had no beneficial effects in MPN, dramatic, but transient, regression of *Nf1*-deficient AMLs was observed (6).

Endogenous expression of oncogenic *Kras* in *Mx1-Cre;Kras*^{G12D} mice causes an aggressive MPN, with death by 4 months of age (5). Interestingly, treatment with PD0325901 (hereafter called 901), a "second generation" MEK inhibitor with optimized pharmacologic properties (8), induced hematologic improvement and greatly prolonged survival in this model of JMML/CMML (9). Remarkably, *Kras*^{G12D} hematopoietic cells persisted after treatment, indicating that MEK inhibition rebalanced growth and differentiation in vivo. We considered 2 general explanations for this unexpected response: (a) there is differential sensitivity of *Nf1* and *Kras* hematopoietic cells to MEK inhibition; or (b) sustained Raf/MEK/ERK pathway inhibition is essential for therapeutic efficacy. To address this question, we administered 901 to *Mx1-Cre;Nf1*$^{flox/flox}$ mice with MPN. Here, we show that treatment with 901 reduces myeloproliferation and enhances erythropoiesis by modulating the behavior of *Nf1* mutant cells in vivo.

Results and Discussion

We first assessed the pharmacodynamic properties of 901 in WT and *Mx1-Cre;Nf1*$^{flox/flox}$ (*Nf1* mutant) mice that received an oral gavage dose of 5 mg/kg/d for 5 days. Mice were euthanized 2, 12, and 24 hours after the final dose, and phosphorylated ERK (p-ERK) levels were measured by flow cytometry in Mac1$^+$ BM cells before and after GM-CSF stimulation (6, 9). GM-CSF induced robust phosphorylation of STAT5 and ERK in cells from untreated *Nf1* mutant mice (Supplemental Figure 1; supplemental material available online with this article; doi:10.1172/JCI63193DS1). Treatment with 901 abrogated ERK activation in BM cells for 12 hours, which was largely restored by 24 hours. In contrast, STAT5 activation was not impaired. A similar pattern of inhibition was observed in multipotent progenitors (c-kit$^+$, lin$^-$, CD48$^-$) (data not shown). In contrast, CI-1040 efficiently inhibits GM-CSF–induced ERK activation for 2–4 hours (6).

We randomly assigned *Mx1-Cre;Nf1*$^{flox/flox}$ mice (n = 35) and their WT littermates (n = 38) to treatment with 901 (at a daily dose of 5 mg/kg) or control vehicle for 10 weeks or until the mice became moribund. Blood leukocyte counts were elevated in *Nf1* mutant mice at entry (Supplemental Figure 2). *Nf1* mutant mice that were treated with 901 had a marked reduction in blood leukocyte

Conflict of interest: The authors have declared that no conflict of interest exists.
Citation for this article: *J Clin Invest.* 2013;123(1):335–339. doi:10.1172/JCI63193.

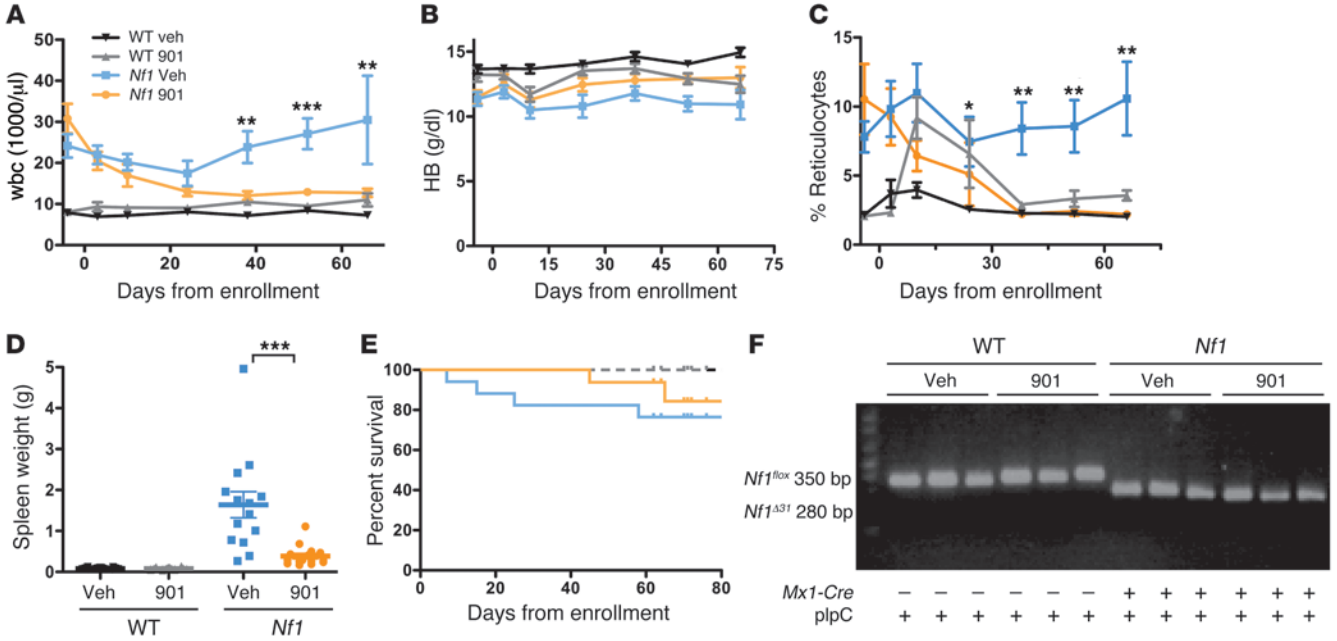

Figure 1

901 reduces myeloproliferation and enhances erythropoiesis in *Mx1-Cre;Nf1*$^{flox/flox}$ (*Nf1*) mice. *Nf1* and WT mice were treated with vehicle (Veh) or 901 for 10 weeks. (**A**) wbc counts, (**B**) hemoglobin (HB) concentrations, (**C**) and percentage of reticulocytes in the blood of *Nf1* mice given vehicle (blue) or 901 (orange) and of WT mice treated with vehicle (black) or 901 (gray). (**D**) Spleen weights at the end of the trial. Mean and SEM are shown (n = 11–13 per group). Asterisks indicate significant differences between *Nf1* mice that received 901 and vehicle (*P < 0.05; **P < 0.001; ***P < 0.0001). (**E**) Kaplan-Meier analysis revealed a trend toward enhanced survival in 901-treated Nf1 mice (P = NS). (**F**) PCR amplification of BM DNA from individual WT and *Nf1* mice at the end of the trial (n = 11–13 per group). Notably, both 901- and vehicle-treated *Nf1* mutant mice demonstrated complete excision of exon 31.

counts, enhanced erythropoiesis, and markedly smaller spleens by the end of the trial (Figure 1, A–D). Whereas most *Nf1* mutant mice survived (Figure 1E), mice assigned to the vehicle group were disheveled and losing weight by the end of the trial, while the 901-treated mice appeared well. Remarkably, we observed complete excision of exon 31 in the BM of both 901- and vehicle-treated *Nf1* mutant mice that completed the trial (Figure 1F). These data indicate that MEK inhibition modulates the behavior of *Nf1* mutant cells in vivo, but does not eradicate them.

Progressive anemia with elevated reticulocyte counts and massive splenomegaly suggested that *Mx1-Cre;Nf1*$^{flox/flox}$ mice with MPN have ineffective erythropoiesis. To investigate this possibility, we grew erythroid burst-forming unit (BFU-E) and CFU (CFU-E) colonies from the BM and spleens of 6-month-old WT and *Nf1* mutant littermates. BM cells from *Nf1* mutant mice that received the vehicle formed greater numbers of BFU-E and CFU-E colonies than the WT controls (Supplemental Figure 3, A and B). We observed more dramatic effects of *Nf1* inactivation in the spleen, with erythroid colony numbers increased 30-fold in *Nf1* mutant mice (Figure 2, A and B). In addition to greatly decreasing splenomegaly (Figure 1D), treatment with 901 reduced the frequency of splenic BFU-E and CFU-E colonies and of BM CFU-E to near-normal levels and reverted splenic histology toward normal (Figure 2, A and B, and Supplemental Figure 3).

Erythroid precursors progressively downregulate the transferrin receptor (CD71) and increase Ter119 expression as they mature from proerythroblasts (region I; Ter119^{lo}CD71^{hi}) to late erythroblasts (region IV; Ter119^{hi}CD71^{lo}) (10). In WT mice, most splenic erythroid cells are late erythroblasts (region IV). In striking contrast, profiling revealed a largely inverted ratio of early-to-late erythroblasts in *Mx1-Cre;Nf1*$^{flox/flox}$ mice, with 10-fold expansion in the percentage of cells in region II, and a reciprocal decline in the number of erythroblasts progressing to region IV (Figure 2C). Treatment with 901 alleviated this block and restored a normal pattern of erythroid differentiation (Figure 2C).

To further characterize the hematopoietic compartment in *Mx1-Cre;Nf1*$^{flox/flox}$ mice with MPN, we enumerated KLS (c-Kit^{+}lin^{-} Sca-1^{+}) cells and myelo-erythroid progenitor populations by flow cytometry (11, 12). The spleens of *Nf1* mutant mice were heavily infiltrated with KLS and myeloid lineage cells at all stages of differentiation with extensive expansion of the megakaryocytic/erythroid progenitor (MEP) compartment (Supplemental Figure 5A). While progenitor populations were also broadly increased in the BM of *Nf1* mutant mice, significant differences were only observed in the number of KLS and pregranulocytic/macrophage (pre-GM) cells (Supplemental Figure 5B). The expanded KLS population (Supplemental Figure 4, A and C) likely includes cells that are required for leukemia initiation and maintenance.

We compared the short- and long-term effects of MEK inhibition on hematopoiesis in *Nf1* mutant mice that received 901 for 5 days or 12 weeks. Treatment induced a significant reduction in the number of splenic myeloid progenitors, which was evident as soon as 5 days after initiating treatment (Figure 3, B and C, and Supplemental Figure 5A). MEK inhibition also reduced the percentages of BM and splenic pre-GM progenitors in *Nf1* mutant mice at both time points and normalized the ratio of pre-GM to

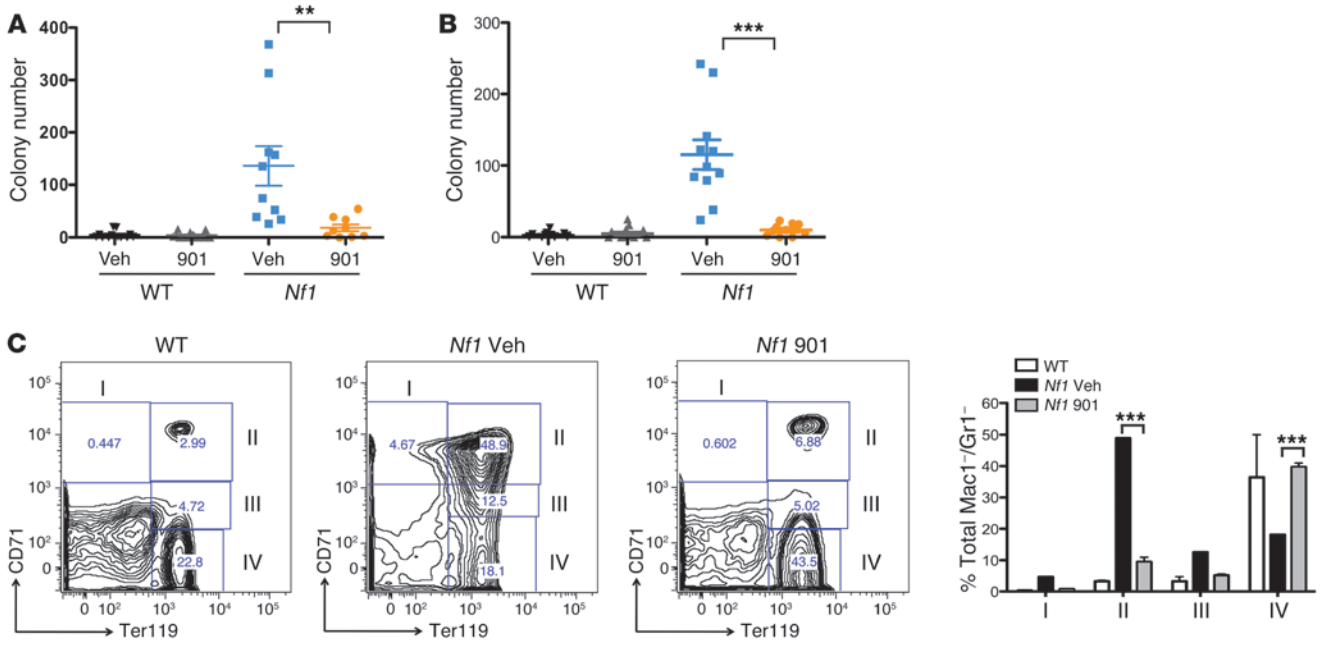

Figure 2

901 restores normal erythroid differentiation in vivo. Hematopoietic tissues from 6-month-old *Mx1-Cre;Nf1*$^{flox/flox}$ (*Nf1*) and WT mice treated with 901 or vehicle were analyzed at the end of the trial. (**A**) BFU-E and (**B**) CFU-E colonies were grown from splenocytes in methylcellulose medium–containing erythropoietin (100 ng/ml). Mean and SEM are shown (n = 11–13 per group). (**C**) Erythroid differentiation was analyzed by flow cytometry using the cell-surface markers CD71 and Ter119. Contour plots of splenocytes from representative WT and *Nf1* mutant mice that were treated for 12 weeks are shown. The relative number of cells in each region as a percentage of viable, nucleated erythroid cells is shown at the far right. The error bars show SEM (n = 5–6 per group), and asterisks indicate significant differences between these groups (**P < 0.001;***P < 0.0001).

pre-megakaryocyte-erythroid progenitor (pre-MegE) cells (Figure 3B and Supplemental Figure 5B). Interestingly, while we also observed reduced numbers of KLS cells after 12 weeks of 901 treatment, there was no significant change at 5 days (Figure 3C). This observation raises the possibility that immature *Nf1*-deficient progenitors and HSCs are less dependent on the Raf/MEK/ERK cascade to maintain a growth advantage, which is consistent with persistence of mutant cells in 901-treated mice despite dramatic hematologic improvement (Figure 1).

Our data show that *Nf1* inactivation perturbs erythropoietic differentiation and alters early progenitor populations in vivo. Additional investigation is required to address the consequences of *Nf1* inactivation on signal transduction and the functional properties of expanded stem and early progenitor populations. We also demonstrate that sustained MEK inhibition results in durable hematologic improvement in this accurate model of JMML. These results were somewhat unexpected, as a previous study of CI-1040, a MEK inhibitor with a much shorter duration of action, was ineffective in *Mx1-Cre;Nf1*$^{flox/flox}$ mice with MPN. We therefore considered the possibility that the enhanced response to 901 might be due to off-target effects. To address this question, we engineered a point mutation that alters the allosteric site in MEK where CI-1040 and 901 bind and results in an approximately 100-fold increase in IC_{50} (13). Expressing this mutant protein in primary hematopoietic cells rescued myeloid progenitor colony growth and restored ERK activation in the presence of 901, but did not overcome the inhibitory effects of PD098059, a structurally unrelated MEK inhibitor (Supplemental Figure 6, A–C). Together with the very similar chemical structures of CI-1040 and 901 (14), these studies provide strong evidence that the degree and duration of target inhibition is a critical determinant of efficacy in vivo.

In contrast to MPN, highly aggressive AMLs generated by retroviral mutagenesis in *Mx1-Cre;Nf1*$^{flox/flox}$ mice were equally sensitive to CI-1040 and 901 (6). These data support the idea that the mutations that are acquired during progression to AML render leukemia cells more dependent on Raf/MEK/ERK signaling. The distinct clinical and biologic responses to MEK inhibitors in MPN and AML initiated by *Nf1* inactivation have therapeutic implications,as they suggest that early stage and histologically benign NF1-associated neoplasms may respond differently to targeted agents than the advanced multistep cancers seen in many NF1 patients.

The maximal dose of 901 currently administered to humans is equivalent to approximately 1.5 mg/kg/d in mice. The aggressive nature of the *Mx1-Cre;Kras*^{G12D} MPN facilitates rapid comparisons of different drug doses in small cohorts, and we performed a pilot experiment in this strain. Mice treated with either 1.5 or 5 mg/kg/d of 901 showed similar hematologic improvement after 8 weeks, and pharmacodynamic analysis showed suppression of GM-CSF–induced p-ERK activation for at least 12 hours (Supplemental Figure 7).

HSCT only cures approximately 50% of patients with JMML, and this treatment carries a substantial risk of acute toxicities and adverse late effects (2). Based on the efficacy of 901 in accurate mouse models, we advocate initiating clinical trials of MEK inhibition in JMML. The recent discovery of frequent somatic *NF1* mutations in some sporadic cancers also supports evaluating MEK inhibitors in these malignancies. Finally, as CMML shares many clinical and molecular similarities with JMML and is largely refrac-

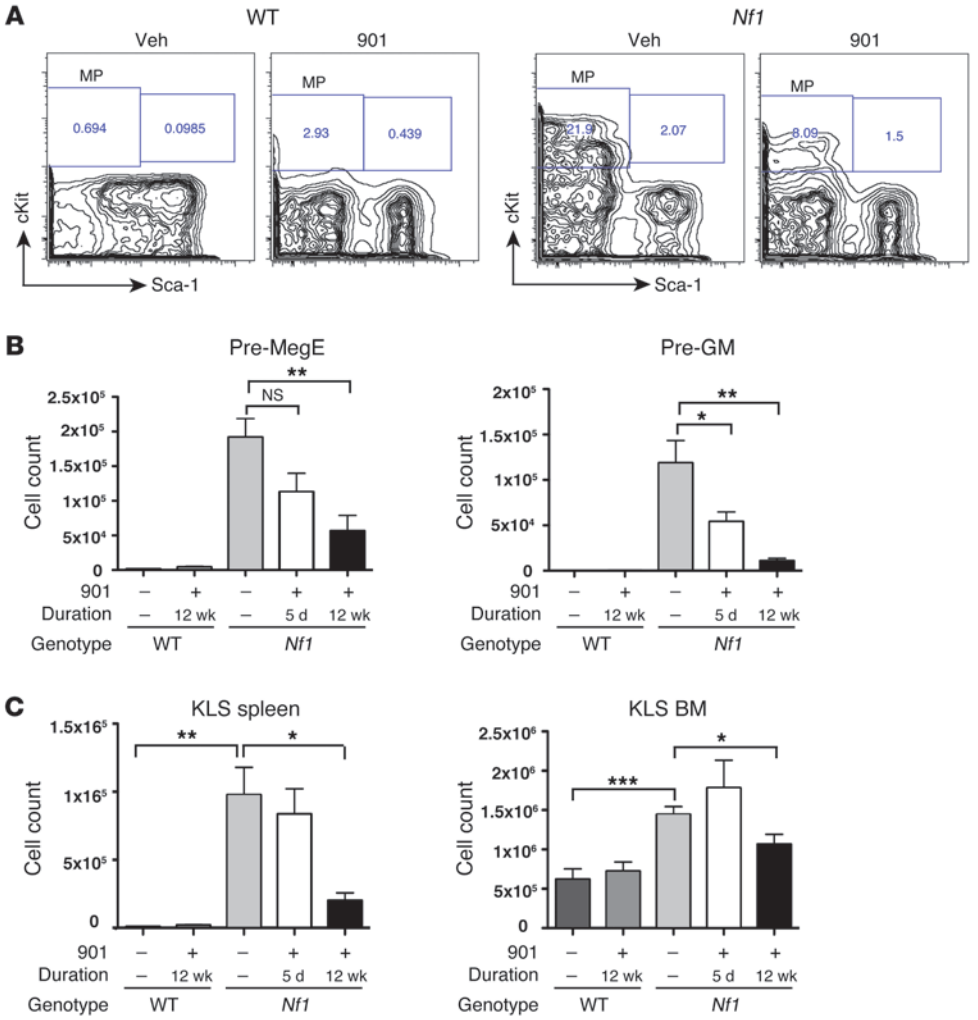

Figure 3
901 normalizes early myelo-erythroid populations in *Mx1-Cre;Nf1*$^{flox/flox}$ (*Nf1*) mice. (**A**) Representative profiles of myeloid progenitors (MP) in the spleens of WT and *Nf1* mice treated with vehicle or 901 for 12 weeks. (**B**) Total numbers of splenic myeloid progenitor cells in WT and *Nf1* mice treated with 901 for 5 days or 12 weeks. (**C**) Total numbers of KLS cells in spleen and BM. In **B** and **C**, the error bars show SEM (n = 5–10 per group), and asterisks indicate significant differences between vehicle-and 901-treated Nf1 mice (*P < 0.05, **P < 0.01, ***P < 0.0001).

tory to current therapies, our data provide a rationale for testing MEK inhibition in this aggressive adult MPN.

Methods

Mice and treatment procedures. *Mx1-Cre;Nf1*$^{flox/flox}$ and control mice were generated and treated with pIpC (Sigma-Aldrich) at 3–5 days, as described previously (9). Mice were randomly assigned to receive either 901 (Pfizer) or hydroxypropyl methylcellulose vehicle by oral gavage once daily. Blood cell and reticulocyte counts were measured using a Hemavet (Drew Scientific) and Retic-Count reagent (BD Biosciences). Mice were euthanized after 10 weeks or when they became moribund.

Flow cytometry. Nucleated BM and spleen cells were stained with the specific antibody combinations indicated in the legend for Supplemental Figure 4 to characterize stem/progenitor populations (11, 12). Intracellular phospho-proteins were analyzed as described (9), with the addition of staining for CD34 and CD105. Data were collected on an LSR II flow cytometer (BD Biosciences) and analyzed with FlowJo (TreeStar).

Progenitor growth. A total of 5 × 10^4 nucleated BM cells or 1 × 10^5 splenocytes were suspended in 1 ml of methylcellulose medium. Erythroid progenitors were grown in M3434 medium (Stem Cell Technologies), and granulocyte-macrophage progenitors were grown in M3231 medium (Stem Cell Technologies) containing recombinant murine GM-CSF (10 ng/ml; PeproTech).

Genotyping. A QIAamp DNA Blood Mini Kit was used to isolate DNA (QIAGEN). Genotyping at the *Nf1* locus was performed using primer 220 sequences and polymerase chain reaction amplification described (15). *Mx1-Cre* genotyping was performed as described previously (16).

Retroviral infections. WT and *L115P MEK* cDNA molecules were cloned into the murine stem cell virus (MSCV), vector with GFP expression driven by the internal ribosomal entry site (IRES). Retrovirally transduced E14.5 fetal liver cells sorted for GFP positivity were plated in methylcellulose to assess CFU-GM growth as described previously (17). Biochemical analyses were performed on cultured macrophages differentiated from transduced GFP-positive fetal liver cells in 50 ng/ml M-CSF as described (17).

Pathologic examination. Paraffin-embedded spleen sections were stained with H&E in the Mouse Pathology Core at the UCSF Comprehensive Cancer Center. Photographs were taken on a Nikon Eclipse 80i microscope with a Nikon Digital Sight camera using NIS-Elements F2.30 software at a resolution of 2560 × 1920. Using Adobe Photoshop CS2, images were set at a resolution of 300 pixels/inch, and autocontrast and unsharp mask were applied.

Statistics. Data were analyzed using Prism 4.0 software (GraphPad). Student's t tests, 2-tailed, unpaired, were used to compare complete blood counts and spleen weights after treatment. Leukocyte counts were log transformed to correct heteroscedasticity; Welsh's correction was applied when variances were unequal. For scatter plots, symbols represent individual samples, horizontal bars represent mean, and error bars show SEM. For

BM and spleen population frequencies and for colony counts, the effects of genotype and treatment cohort were analyzed by 2-way ANOVA, and Bonferroni's post-test comparisons were performed within each population against the WT/vehicle cohort. Kaplan-Meier survival analysis was determined by the log-rank test (Mantel-Haenszel test) with a 2-tailed *P* value. $P < 0.05$ was considered significant.

Study approval. Animal use protocols were approved by the UCSF Committee on Animal Research.

Acknowledgments

We are grateful to Pfizer Inc. for providing PD0325901 to Luis Parada (UT Southwestern) for *Nf1* mutant mice and to Mila McCurrach for facilitating this work through the Neurofibromatosis Preclinical Consortium (NFPC). This work was supported by an NFPC award from the Children's Tumor Foundation; by NIH grant R37 CA72614; by a LLSA Specialized Center of Research grant; and by St. Baldrick's Foundation awards to B.S. Braun and T. Chang. K. Shannon is an American Cancer Society Research Professor.

Received for publication February 1, 2012, and accepted in revised form September 27, 2012.

Address correspondence to: Kevin Shannon, Helen Diller Family Cancer Research Building, University of California, San Francisco, 1450 3rd Street; Room 240, San Francisco, California 94158-9001, USA. Phone: 415.476.7932; Fax: 415.502.5127; E-mail: shannonk@peds.ucsf.edu.

Jennifer O. Lauchle's present address is: Genentech, South San Francisco, California, USA.

1. Cichowski K, Jacks T. NF1 tumor suppressor gene function: narrowing the GAP. *Cell*. 2001; 104(4):593–604.
2. Loh ML. Recent advances in the pathogenesis and treatment of juvenile myelomonocytic leukaemia. *Br J Haematol*. 2011;152(6):677–687.
3. Side L, et al. Homozygous inactivation of the NF1 gene in bone marrow cells from children with neurofibromatosis type 1 and malignant myeloid disorders. *N Engl J Med*. 1997;336(24):1713–1720.
4. Bollag G, et al. Loss of *NF1* results in activation of the Ras signaling pathway and leads to aberrant growth in murine and human hematopoietic cells. *Nat Genet*. 1996;12(2):144–148.
5. Ward AF, Braun BS, Shannon KM. Targeting oncogenic Ras signaling in hematologic malignancies. *Blood*. 2012;120(17):3397–3406.
6. Lauchle JO, et al. Response and resistance to MEK inhibition in leukaemias initiated by hyperactive Ras. *Nature*. 2009;461(7262):411–414.
7. Van Etten RA, Shannon KM. Focus on myeloproliferative diseases and myelodysplastic syndromes. *Cancer Cell*. 2004;6(6):547–552.
8. Brown AP, Carlson TC, Loi CM, Graziano MJ. Pharmacodynamic and toxicokinetic evaluation of the novel MEK inhibitor, PD0325901, in the rat following oral and intravenous administration. *Cancer Chemother Pharmacol*. 2007; 59(5):671–679.
9. Lyubynska N, et al. A MEK inhibitor abrogates myeloproliferative disease in Kras mutant mice. *Sci Transl Med*. 2011;3(76):76ra27.
10. Zhang J, Socolovsky M, Gross AW, Lodish HF. Role of Ras signaling in erythroid differentiation of mouse fetal liver cells: functional analysis by a flow cytometry-based novel culture system. *Blood*. 2003;102(12):3938–3946.
11. Akashi K, Traver D, Miyamoto T, Weissman IL. A clonogenic common myeloid progenitor that gives rise to all myeloid lineages. *Nature*. 2000; 404(6774):193–197.
12. Pronk CJ, et al. Elucidation of the phenotypic, functional, and molecular topography of a myeloerythroid progenitor cell hierarchy. *Cell Stem Cell*. 2007;1(4):428–442.
13. Emery CM, et al. MEK1 mutations confer resistance to MEK and B-RAF inhibition. *Proc Natl Acad Sci U S A*. 2009;106(48):20411–20416.
14. Barrett SD, et al. The discovery of the benzhydroxamate MEK inhibitors CI-1040 and PD 0325901. *Bioorg Med Chem Lett*. 2008;18(24):6501–6504.
15. Zhu Y, et al. Ablation of NF1 function in neurons induces abnormal development of cerebral cortex and reactive gliosis in the brain. *Genes Dev*. 2001; 15(7):859–876.
16. Le DT, et al. Somatic inactivation of Nf1 in hematopoietic cells results in a progressive myeloproliferative disorder. *Blood*. 2004;103(11):4243–4250.
17. Schubbert S, et al. Germline KRAS mutations cause Noonan syndrome. *Nat Genet*. 2006;38(3):331–336.